

Egyptian Journal of Chemistry

http://ejchem.journals.ekb.eg/



Experimental Investigation of Oxyhydrogen Gas Production for Alkaline Water Electrolyzer using Stainless Steel Perforated Plate Type Electrodes



Hamdy H. El-Ghetany*1, Mohamed A. Halawa2, Aml E. Mohammed 2,3,

¹Solar Energy Department, National Research Centre, Dokki, 12622, Giza, Egypt ²Mechanical Engineering Department, Al-Azhar University, Cairo, Egypt ³High institute of engineering, Culture and Science City, 6 October City, Egypt

Abstract

The present work experimentally investigated the Oxy-Hydrogen (HHO) electrolyzer using perforated Stainless Steel (SS) plates electrodes. Several experimental runs are made to find out the optimum conditions for HHO gas generation based on the applied current, voltage and electrolyte concentration rate. Electric current and rate of HHO produced are measured with different Potassium Hydroxide (KOH) concentrations to find out the optimal concentration ratio versus rate of HHO volume production. The experimental set up is installed in the Solar Energy Department, National Research Centre, Dokki, Cairo, Egypt. The system consists of several electrolysis cells, each with a different number of electrodes and neutral plates placed between them to achieve maximum gas generation rate. Both neutral plates and electrodes were prepared from SS 316 L sheet with a thickness of 2 mm and by using a laser cutting machine the perforated shape is made. Different KOH concentrations were used from 5 to 40 wt% in all studied cells. Consequences prove that the production rate of HHO gas has increased significantly by increasing electrolyte concentration, reaching the optimum value at 30 wt% of potassium hydroxide concentration. Moreover, the generation rate of HHO gas using perforated plates is higher than that of solid plates and it was increased as the number of cells and number of neutral plates increased.

Keywords: Perforated electrodes, KOH concentrations, Oxy-hydrogen, HHO electrolyzer, Water electrolysis

1. Introduction

As a result of population growth, the use of cars has expanded dramatically, leading to the excessive use of fossil fuels, and, consequently, the spread of pollution, which must be mitigated by using renewable resources [1]. From this standpoint, Oxy-Hydrogen (HHO) gas is considered as an altrenative encouraging fuel that offers multiple features such as zero carbon emissions, rapid combustion rate, high oxygen content, and superior inflammability [2] [3]. Therefore, HHO gas has the capability to solve the problem of petroleum fuel deficiency as is used in internal combustion engines, metal cutting, welding [4] [5]. In the alkaline electrolytic medium, the chemical bond between H₂ and O₂ is broken by electrical energy generated by an electrolyzer. As a result, the molecules of water are divided into oxygen and hydrogen by using a diaphragm as shown in equation (1), with minimum emissions of greenhouse gases. But, in the absence of this diaphragm, oxygen and hydrogen gases combined to form oxy hydroxy gas, which provides an auxiliary fuel [6].

$H_2O_{(l)} + Electric Energy \longrightarrow H_{2(g)} + 0.5 O_{2(g)}$ [1]

When the current density is higher, the alkaline electrolysis efficiency becomes better, by reducing the energy losses caused by gas bubbles and ohmic losses [7–10]. Bubbles from oxygen and hydrogen gases cause losses, resulting in a decrease in the electrolyte conductivity and clogging of the electrodes active area [11-13]. These bubbles take up most of the volume of the electrolyzer causing energy losses. Therefore, perforated electrodes are recommended to be used to facilitate the passage of gas and water [14] [15]. Therefore, a zero-gap alkaline water electrolysis cell having different types of electrodes should be used [16,17], such as perforated [18], foam [19], and mesh electrodes [20]. The electrical conductivity of the electrolyte solution must be increased to efficiently generate hydroxy gas. Therefore, a mixture of distilled water and a catalyst can be used as an electrolyte solution. Various catalysts are available, but the most favorable type is Potassium Hydroxide (KOH), because it is compatible with metal components. Numerous technologies for generating hydrogen and their ecological impacts have been investigated in [21]. A significant amount of carbon emissions is produced from the Steam Methane Reforming (SMR) process. Therefore, carbon must be stored and captured using new techniques to reduce the undesirable ecological impacts, irrespective of their high production rate and cost effectiveness. Electrolysis needs sources of renewable energy to produce more efficient energy. Converting biomass to gas produces no carbon emissions but is less energy efficient. Finally, each method has advantages and disadvantages in terms of ecological impacts, affordability, scalability, and performance.

For minimizing ecological pollution and fuel consumption, hydroxy gas can be used for vehicles and other applications in the society. In this regard, the parameters affecting the hydroxy gas generators were studied in [5] using water electrolysis with a

*Corresponding author e-mail: hamdy.elghetany@gmail.com; (Hamdy El-Ghetany). Received Date: 21 June 2025, Revised Date: 29 July 2025, Accepted Date: 17 August 2025

DOI: 10.21608/EJCHEM.2025.396452.11934

dry fuel cell. These parameters include concentration of the electrolyte with range being 0.05 - 0.20 M, and applied voltage with range being 10.5 - 13 V. The optimal concentration of KOH and applied voltage range for hydroxy gas generation are 0.05 - 0.10 M, and 11.5 -12 V respectively. In this case, there is 53.79% generator efficiency, 3.43 kWh/m³ specific energy, and the highest productivity is 343.9 cm³/min at electrolyte concentration of 0.10 M and applied voltage of 12 V. Therefore, modifying parameters affecting HHO gas generators is critical to generate HHO gas efficiently. HHO gas generation using a dry cell hydroxy generator was reported in [22], where electrolytes concentration, electrolyte types, plate configurations, and material types of electrodes were studied. Results revealed that the solution conductivity is directly proportional to the electrolyte's concentration. Compared with Sodium Bicarbonate (NaHCO₃) and NaOH, KOH is the most suitable electrolyte for generating HHO gas. On the other hand, the appropriate conductive electrodes than graphite, copper and iron are stainless steel, due to the absence of deposits during electrolysis and have excellent resistance to electrical corrosion. Also, adding more neutral plates and electrodes will maximize the gas generation rate, lessen the gap between electrodes and enlarging their cross-sectional area, will increase the operating current and the HHO gas production rate. Dry cells offer more benefits than wet cells and greater safety. Hydroxy generator efficiency and discharge are affected by the holes that are punched on the electrodes. Therefore, sets of 2, 4, and 9-hole perforated electrodes were fabricated and used to demonstrate the HHO gas generator performance, it is found that hole's numbers are directly proportional to the efficiency and HHO gas production rate [23]. Power consumption rises at the beginning of the process, reaches a peak value, and then decreases over time. Developing and fabricating a dry cell type HHO gas generator featuring high energy-conversion efficiency using locally obtainable materials, and ease of manufacturing is the major objective of the present work. Numerous parameters impacting the hydroxy gas generator performance have been studied.

2. Experimental Setup

2.1 Design and Fabrication of HHO Cells System

The experimental setup shown in figure 1 consisted of several electrolysis cells, mounted on a test-rig, each with a different number of electrodes and neutral plates placed between them to achieve maximum gas generation rate. Each cell has an inlet valve for the electrolyte solution to enter, and an outlet valve for the HHO gas to exit. The cells are connected to three tanks, storage tank containing the electrolyte solution, which is fed into the cells through water valves. The second tank receives HHO gas coming out of the cells through the water valves with some drops of water. The water droplets went down to the bottom of the tank, while the HHO gas is directed to the third tank (bubbler tank) which acts as gas storage. If there are some drops of water inside the bubbler tank, they are transferred back to the storage tank. The HHO gas exits the bubbler tank heading towards the production rate measuring device. Electric panel with several on-off switches for each cell is installed to provide the required electrical current for each cell to for the electrolysis process.

2.2 Manufacturing HHO Cells

The HHO generator was designed and manufactured as shown in figure 2. It consists of several parts, such as two base plates made of heat-resistant acrylic plastic (cell frame) with dimensions of 24.4 cm x 24.4 cm with a thickness of 8 mm that acts as housing for the HHO cell. One acrylic plate has been punched from the lower, and the other from upper, to allow the electrolyte to enter and the gas to exit, respectively. For the electrodes and neutral plates, 316 L perforated SS square plates of 150 mm x 150 mm and 2 mm thick are used according to their suitable characteristics as shown in figure 3. Bubbles from oxygen and hydrogen gases cause energy losses, resulting in a decrease in the electrolyte conductivity and clogging of the electrodes active area. Therefore, perforated electrodes are used to facilitate the passage of gas and water. Care must be taken to avoid contact of neutral plates by electrodes, therefore, neutral plates were cut from the two upper edges, while electrodes were cut from only one upper edge. Furthermore, electrodes were drilled from the lower and upper middle by 13 mm for allowing the electrolyte to enter and the gas to exit. There is also another 10 mm diameter hole made in the electrodes upper edge to conduct the electric charge across two rods. Among the electrodes were rubber gaskets with the same dimensions as the electrodes. These gaskets are made of corrosion resistant rubber, preventing adjacent plates from touching each other as shown in figure 4. An air tube elbow connectors fixed to the cell frame are used as the cell electrolyte inlet and gas outlet. These connectors are connected to a silicon hose with 12.5 mm diameter for receiving the electrolyte and releasing the gas. Nails or screws were used to connect the two acrylic plates containing stainless steel plates inside. They should be tightened gently to prevent electrolyte or gas leakage and to avoid tearing any of the acrylic plastic covers. On the other hand, KOH was mixed with purified water to obtain high electrolytic conductivity and raise the flowing current. Figure 5 shows the manufactured system of the HHO gas generator comprises acrylic plates, rubber gaskets, electrodes, electrical wires, pneumatic connectors, hoses, and screw nuts are used to connect the generator structure.

2.3 Experimental Procedure

The cells installed on the test rig will be tested in terms of the HHO production rate. The test is carried out for each cell separately based on the concentration rate of the electrolyte solution as each cell differs from the other according to the number of electrodes and perforated SS plates placed between electrodes to distribute the gas. Therefore, each tested generator was labelled, for example 2C 4N, where "C" and "N" refer to the number of cells and neutral plates within the generator. Thus, the first cell has solid plates 1C 1N, the second cell has perforated plates 1C 1N, the third cell has perforated plates 1C 2N, the fourth cell has perforated plates 1C 3N, the fifth cell has perforated plates 2C 2N, and the sixth one has perforated plates 2C 3N. At the beginning of the experiment, the electrolyte solution must be prepared at a desired concentration. Since KOH is the catalyst that can be used, a digital electrical balance of one gram accuracy is used to weigh it.

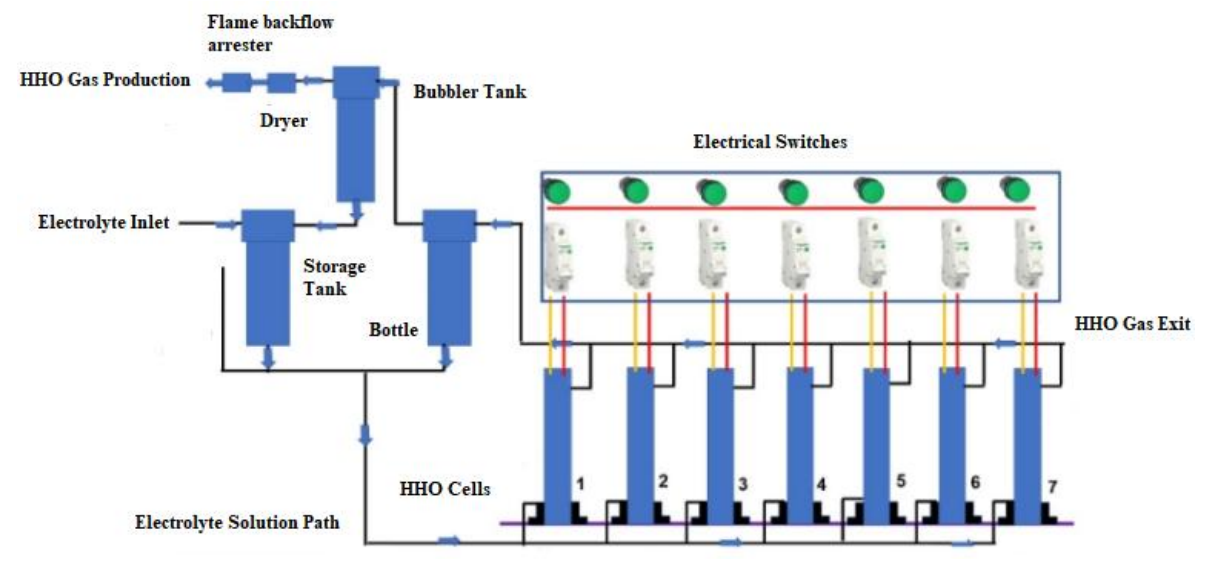


Figure 1: HHO gas generators system.

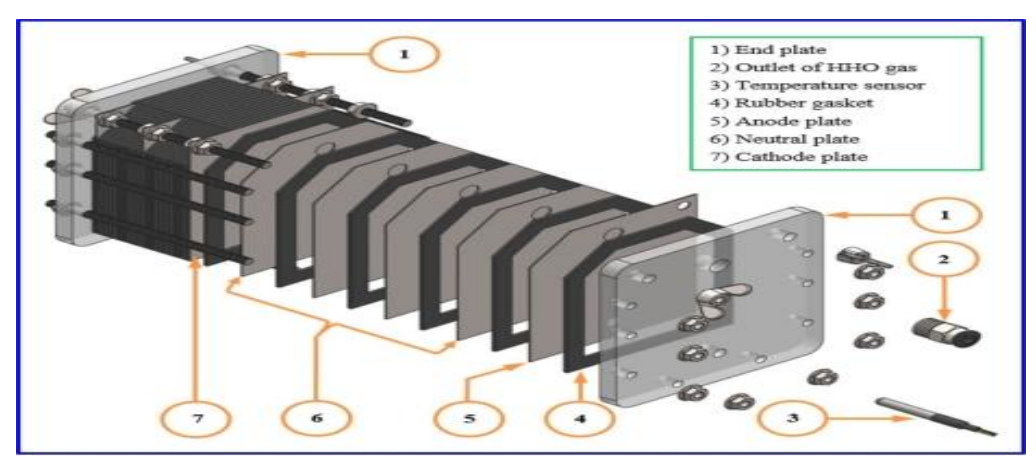


Figure 2: Assembly drawing of HHO gas generator structure [5].



Figure 3: (a) Solid electrode and neutral plates, (b) Perforated electrode and neutral plates.

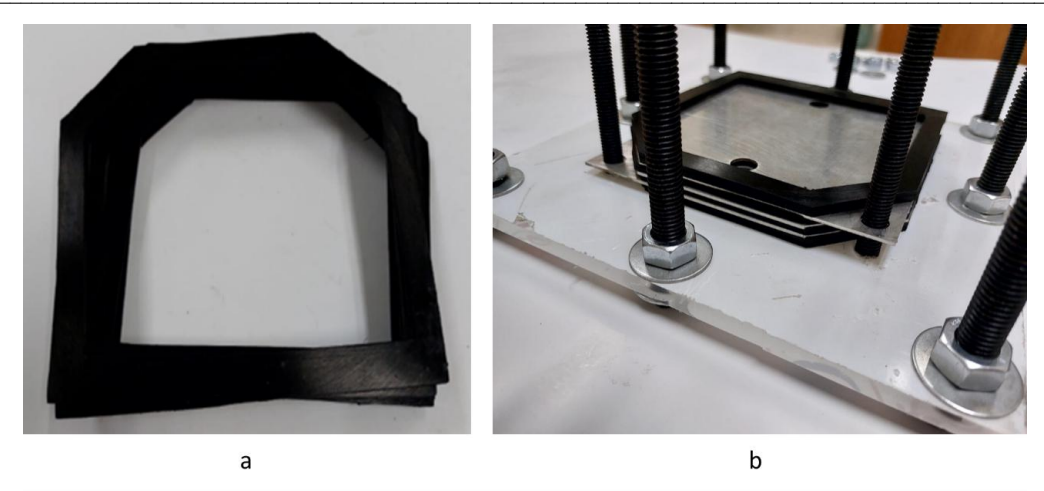


Figure 4: (a) Rubber Gaskets used, (b) Position of the rubber gaskets inside the cell.

A measurable KOH quantity is mixed with one Liter of pure water to provide a highly conductive electrolyte, which is then poured into an HHO gas generator. Thus, a homogeneous solvent was obtained. The potassium hydroxide percentage used is six levels 5, 10, 15, 20, 25, 30, 35 and 40 wt%. The level of electrolyte is located approximately 15 mm below the gas orifice. The HHO cell is powered by a 12V-DC battery which is charged from solar photovoltaic system. When an electric current flows, water molecules decompose, with the negative electrode collecting hydrogen gas, while the positive electrode collects oxygen gas. There is a combination of one-third oxygen and two-thirds hydrogen bound with each other, then rising out of the cell. Table 1 displays the overall descriptions of the constructed HHO gas generator.

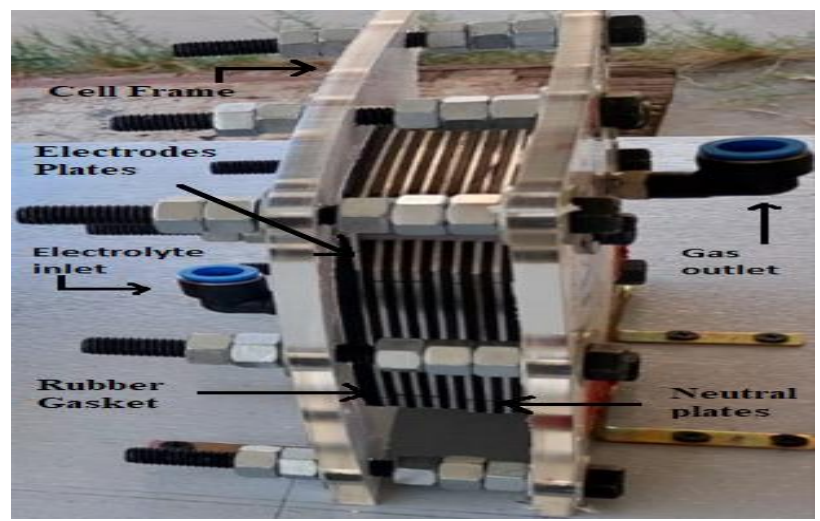


Figure 5: Manufactured HHO gas generator.

Table 1: Descriptions of the Constructed Electrolyzer

Table 1. Descriptions of the Constituted Electroryzer	
Factors	Specifics
Type of HHO generator	Dry cell
Main dimensions of the cell frame	240 x 240 x 80 mm
Electrodes and neutral plates	316 L Stainless steel
Main dimensions of the perforated	150 x 150 x 2 mm
electrodes and neutral plates	
Gasket's thickness	2 mm
Plate design	(1C 1N) S, (1C 1N) P, (1C 2N) P, (1C 3N) P,
_	(2C 4N) P, (2C 3N) P
Input DC voltage	12 V–DC
Catalyst of electrolyte	КОН
Type of water	Distilled water

Reactions taking place are as follows [24]:

Cathode (reduction) reaction:
$$2H_2O + 2e^- \rightarrow H_2 + 2OH$$

Cathode (reduction) reaction:
$$2H_2O + 2e^- \rightarrow H_2 + 2OH$$
 [2]
Anode (oxidation) reaction: $4OH \rightarrow O_2 + 2H_2O + 4e^-$ [3]

Overall reaction: $2H_2O \rightarrow 2H_2(g) + O_2(g)$

The equipment and tools used in the present work, and the experimental setup are shown in Figure 6 and 7, where the cells on the test rig are fed with the KOH electrolyte solution from the storage tank. The HHO gas liberated from the cells is then discharged into the bubbler tank through water valves towards the HHO production rate measuring device to measure the HHO gas flow rate. The generated HHO gas was evaluated via movement of water below atmospheric pressure. HHO gas comes out the bubbler tank and rises into the open water pool, forcing water down into the inverted graduated cylinder. The volume of gas collected in the graduated cylinder per unit of time was measured as the HHO flow rate. Therefore, to evaluate the performance of the HHO gas generator, the productivity of HHO gas generator can be calculated from the following equation (5):

$$Q_g = \frac{V_{HHO}}{t}$$
 [5]

Qg: is the productivity of HHO gas generator (Liter/min)

V_{HHO}: is the volume of HHO gas (Liter)

T: is the operating time (min)

The specific energy requirement [Es (W min/L)] was calculated by using the following equation [5]:

$$E_{g} = \frac{P}{Q_{g}} \tag{6}$$

where P is the consumed power (W) and Qg is the productivity of HHO gas



Figure 6: Raw materials and tools used in the present work



Figure 7: Experimental Setup of HHO gas generator.

Faraday Efficiency

At electrodes, the rate of electron transfer affects the H₂ production, according to faraday's law, which is proportional to the external circuit electrical current. Conversely, in the electrolyzer, the highest practical to theoretical volume of H₂ generated, is called Faraday's efficiency. In terms of temperature, the higher the temperature, the lower the resistance, the lower the Faraday's efficiency, and the higher the current losses, which can be shown by equation [7].

$${}^{\eta}_{F} = \left[\left(\frac{I}{A_{ele}} \right)^{2} / f_{1} + \left(\frac{I}{A_{ele}} \right)^{2} \right] f_{2}$$
 [7]

According to the above equation, f1 and f2 are constant values, while (I) is the current flowing through the HHO generator. On the other hand, from figure 3, the area of electrodes will be calculated by subtracting the area of holes (Aholes) drilled in the perforated plates, the area of the cutt-off part from the electrodes upper edges (Acut) to avoid contact of neutral plates by electrodes, and the area of the holes drilled for electrolyte inlet and gas outlet (Aele. in & gas out) from the total area.

Where

Aele = Atotal - Aholes - Acut - Aele. in & gas out
$$A_{\text{holes}} = \frac{\pi}{4} D_{\text{hole}}^{2} * \text{number of holes}$$

$$A_{\text{out}} = 2 * [0.5 * 1.8 * H]$$
[10]

$$A_{\text{cut}} = 2 * [0.5 * L * H]$$
 [10]
Aele. in & gas out = $2 * \frac{\pi}{4} D^2$ [11]

ele. in & gas out =
$$2 * \frac{\pi}{4} D^2$$
 [11]

 $f_1 = 200 \text{ (mA}^2/\text{cm}^{-4})$

 $f_2 = 0.985$

Based on these data, the faraday efficiency value is 0.98

Polarization resistance (Rp)

Polarization resistance (Rp) of a corroding metal is defined using Ohm's Law as the slope of a potential (E) vs current density (log i) plot at the corrosion potential (Ecorr). Here $Rp = (\Delta E)/(\Delta I)$ at E=0. By measuring this slope, the rate of corrosion can be measured. The correlation between i_{corr} and slope (dI)/(dE) is given by [25] [26]:

$$R_{p} = \frac{\Delta E}{\Delta I} = \frac{\beta_{a}\beta_{c}}{2.3 i_{corr} [\beta_{a} + \beta_{c}]}$$
[12]

Where i_{corr} is the corrosion current density [mA/cm²], and β_a and β_c are Tafel slopes.

Corrosion rate (CR)

The corrosion rates are generally monitored using the Linear Polarization Resistance (LPR) method, via a computer-controlled interface system and is given by [25] [26] [27]:

$$CR = C. \frac{M i_{corr}}{n \rho}$$
 [13]

For 316L stainless steel

 ρ : is the density = 8 (g/cm³)

i_{corr}: is the corrosion current density (mA/cm²)

M: is the atomic weight = 55.8 (g/mol)

n: is the number of electrons involved = 2

C: is a constant value = 3.27

On the other hand, corrosion rate is given as the decrease in thickness per time unit according to the corrosion that has occurred, and thus, the life of the 316L stainless steel is determined by [26]:

SS Lifetime =
$$\frac{t}{CR}$$
 [14]
Where (t) is the electrode thickness

3. Results and Discussion

The oxy-hydrogen generation system operated by a photovoltaic module was experimentally investigated to achieve a high flow rate of HHO gas by means of the most suitable factors.

3.1 Effect of Electrolyte concentrations

The performance of the HHO generator depends greatly on the electrolyte conductivity, so, specifying the electrolyte catalyst concentration is very sensitive because the gas generation process is more efficient if the concentration is high. But, if the concentration exceeds the required limit, it leads to severe corrosion of the electrodes. Thus, the appropriate concentration

Egypt. J. Chem. 69, No. 2 (2026)

relies on the electrolyte catalyst type. Because potassium hydroxide is a powerful catalyst, it can be used in this work using 5-40 wt%. Results demonstrated that, at approximately 30 wt% of KOH, the HHO gas flow rate and the flowing current were in a highly efficient state. This means that the pure water was saturated with potassium hydroxide at this percentage and reached its highest conductivity. In other words, the generated hydroxy gas increased gradually with increasing the KOH concentration and when the concentration exceeds 30 wt %, the flow rate of HHO gas begins to decrease. Figure 8 presents the behavior of the 1C-1N solid generator at various concentrations. As can be seen, the HHO gas flow rate was recorded at 30 ml/min at 30 wt %, and 17.6 ml/min at 5 wt %, which are the maximum and minimum values flow rate, respectively. Figure 9 presents the behavior of the 1C-1N solid generator at various concentrations. It can be observed that the flowing current was recorded 3.5 A at 30 wt %, and 2.3 A at 5 wt %, which are the maximum and minimum values of current, respectively. It can be concluded that, until the concentration reaches 30 wt %, corrosion of SS does not occur, this indicates an optimal conductivity of this electrode material.

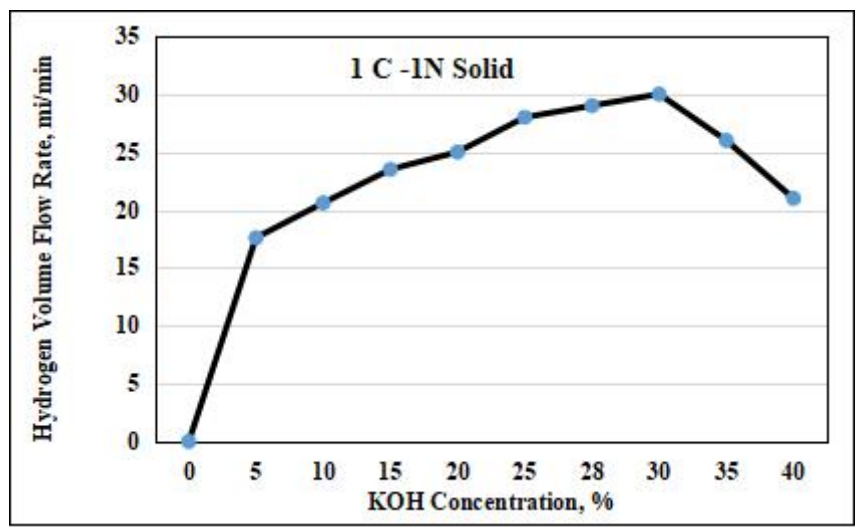


Figure 8: Behaviour of the 1C-1N solid generator at various concentrations as a function of HHO gas flow rate.

Regarding previous research, A. Ramadan [28] demonstrated that at 30 wt % of KOH, the hydrogen gas flow rate and the flowing current were in a highly efficient state using a dry cell. While at this concentration, the hydrogen gas flow rate and the flowing current were recorded as 27.5 ml/min and 3.1 A respectively, which are the highest values for both. It can be concluded that these data are consistent or nearly close with the reported data in the present work as shown in Figure 10 and

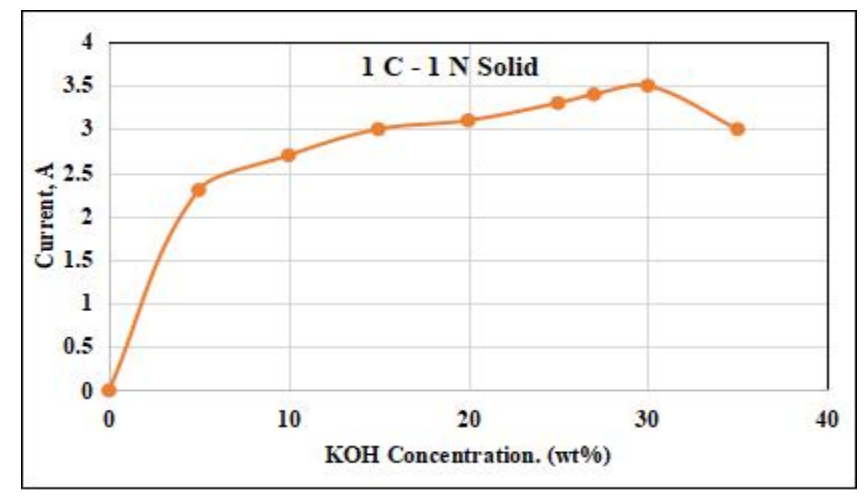


Figure 9: Behaviour of the 1C-1N solid generator at various concentrations as a function of flowing current.

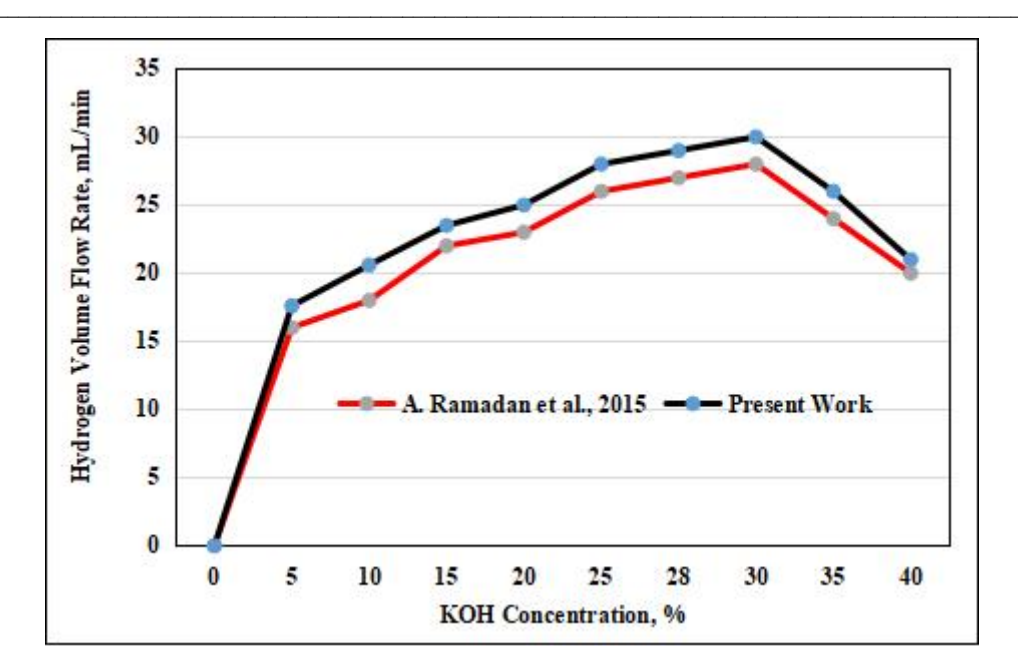


Figure 10: Behaviour of the electrolyzer cell at various concentrations as a function of hydrogen volume flow rate for 1C-1N solid cell and A. Ramadan et al., 2015.

The optimal KOH concentration range for hydroxy gas generation is 5 - 30 wt%. At this concentration range, The range of HHO gas flow rate for the (1C 1N) P, (1C 2N) P, (1C 3N) P, (2C 4N) P, (2C 3N) P generators are 275.35 - 688.35 ml/min, 285 - 780.6 ml/min, 300 - 915.5 ml/min, 350 - 1100.4 ml/min, and 384 - 1210 ml/min respectively, as shown in figures 12 to 16

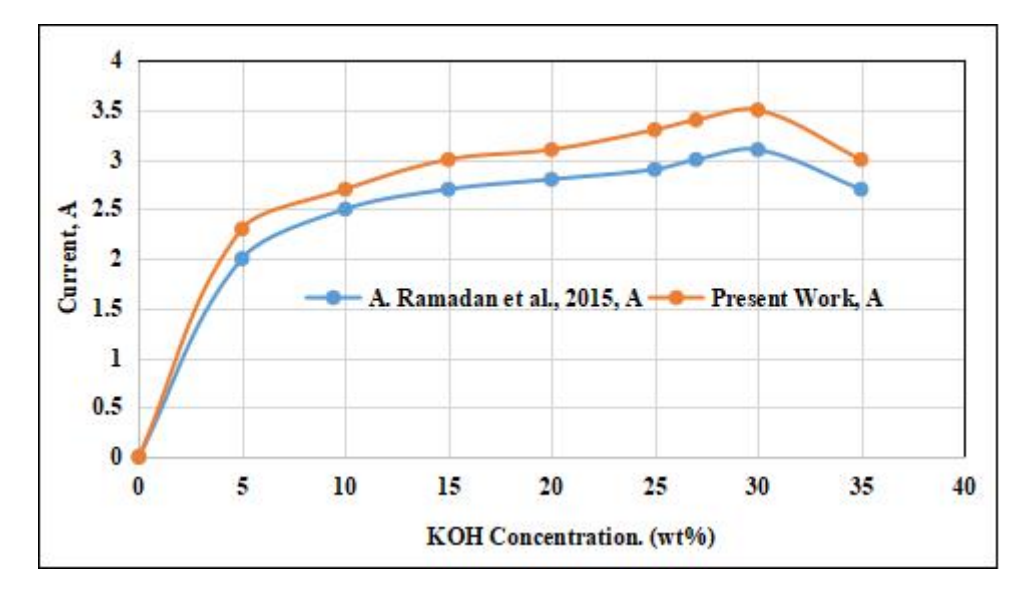


Figure 11: Behaviour of the electrolyzer cell at various concentrations as a function of flowing current for 1C-1N solid cell and A. Ramadan et al., 2015.

It can be concluded that the generated hydroxy gas increased gradually with increasing the KOH concentration and when the concentration exceeds 30 wt%, the flow rate of HHO gas begins to decrease because severe corrosion of the electrodes will occur after the concentration reaches 30 wt%.

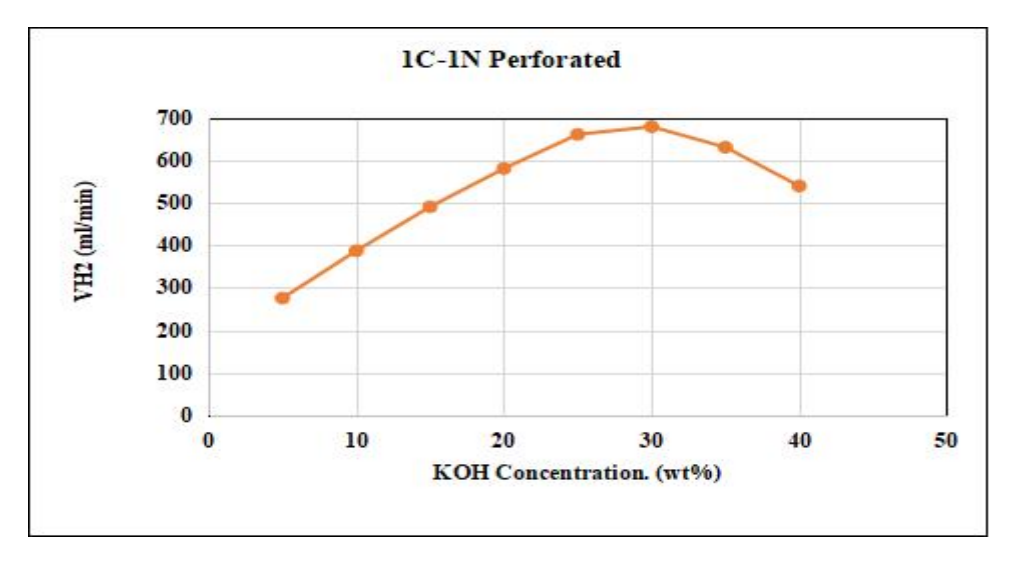


Figure 12: Behaviour of the 1C-1N perforated generator at various concentrations as a function of HHO gas flow rate.

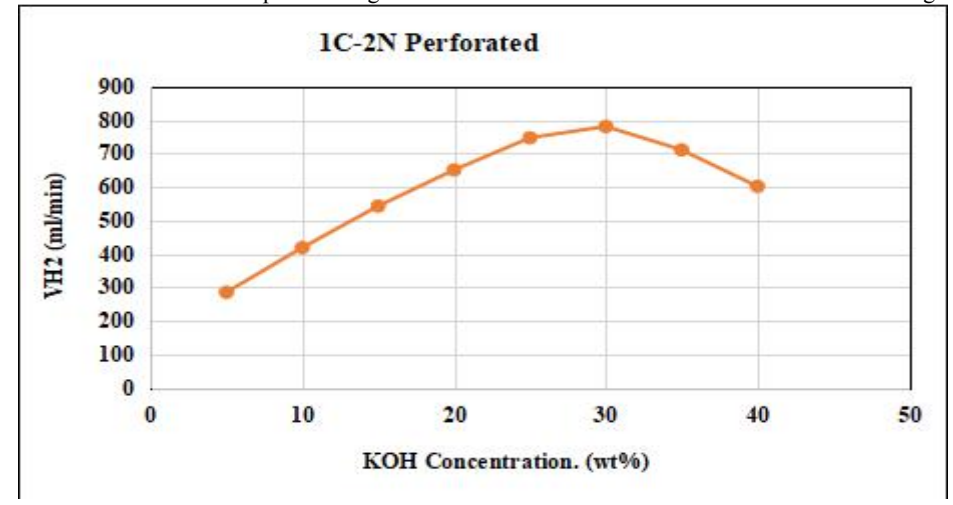


Figure 13: Behaviour of the 1C-2N perforated generator at various concentrations as a function of HHO gas flow rate.

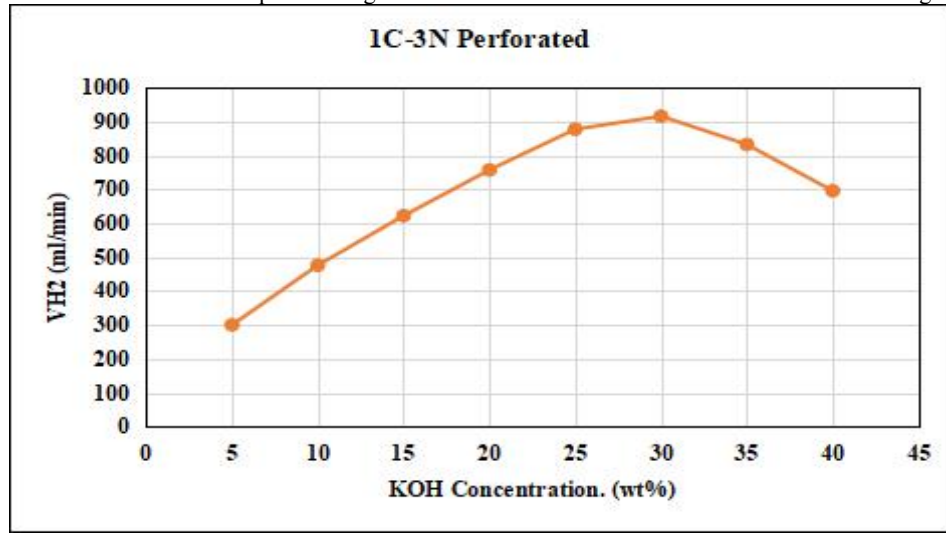


Figure 14: Behaviour of the 1C-3N perforated generator at various concentrations as a function of HHO gas flow rate.

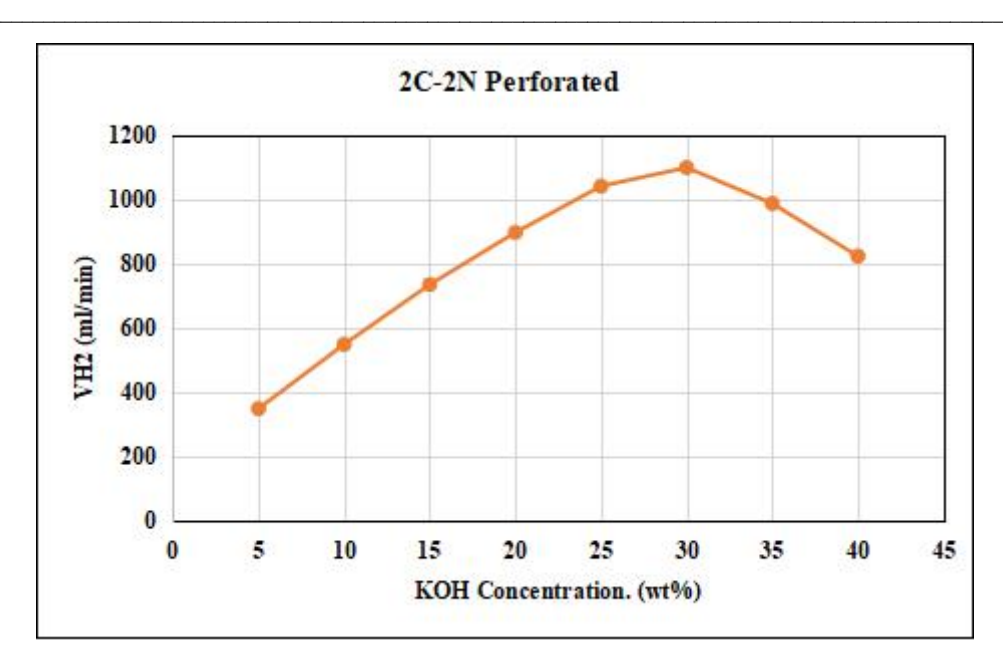


Figure 15: Behaviour of the 2C-2N perforated generator at various concentrations as a function of HHO gas flow rate.

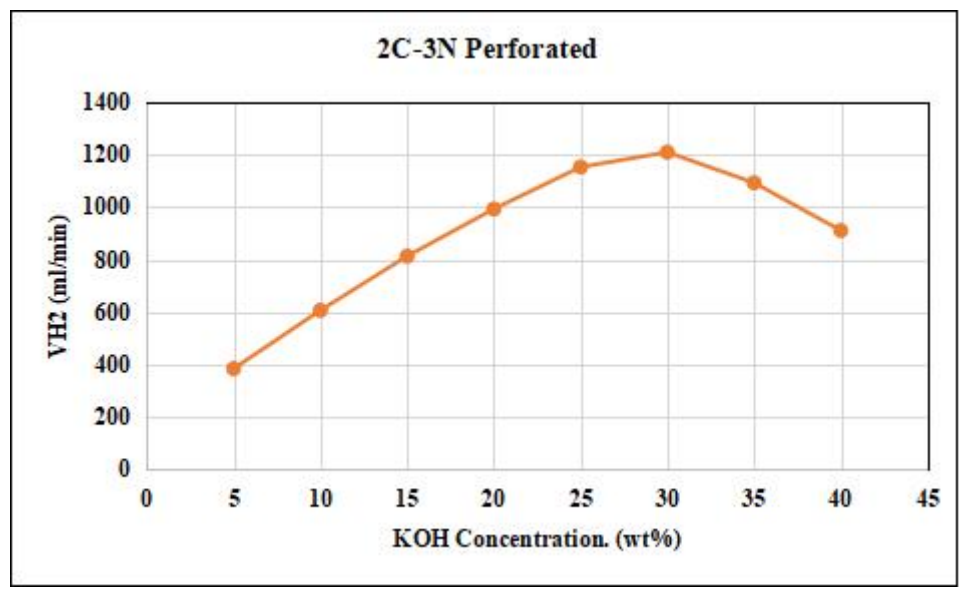


Figure 16: Behaviour of the 2C-3N perforated generator at various concentrations as a function of HHO gas flow rate.

Figures 17 and 18 show the behaviour of all cells at various concentrations as a function of HHO gas flow rate and flowing current. It can be concluded that both hydroxy gas flow rate and current are directly proportional to the KOH concentration up to reaches 30 wt%. The HHO gas flow rate and flowing current values for 2C-3N perforated generator were recorded as 1210 ml/min and 46 A respectively 30 wt%. Where the HHO gas flow rate and flowing current values for 1C-1N solid generator were recorded as 688.35 ml/min and 3.5 A respectively 30 wt%. This means increasing the number of cells and perforated plates results in more HHO gas being generated.

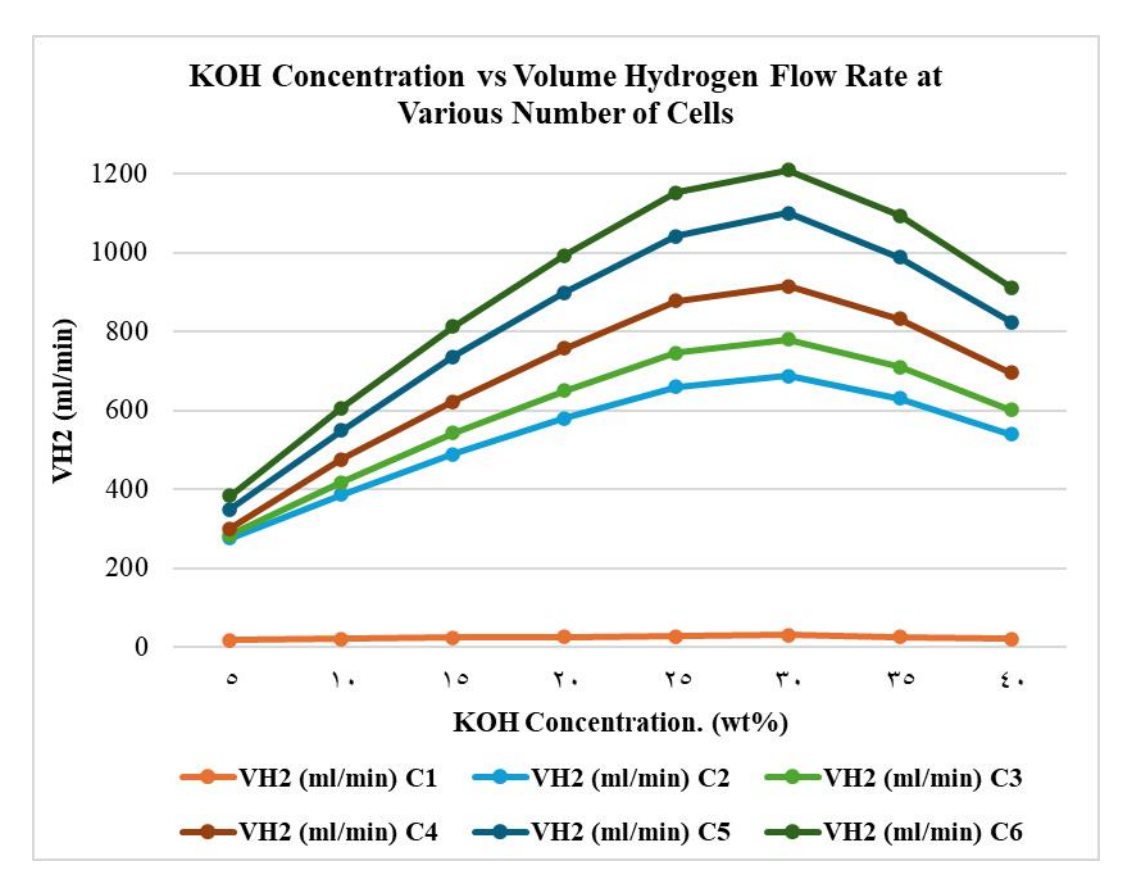


Figure 17: Behaviour of solid and perforated cells at various concentrations as a function of HHO gas flow rate.

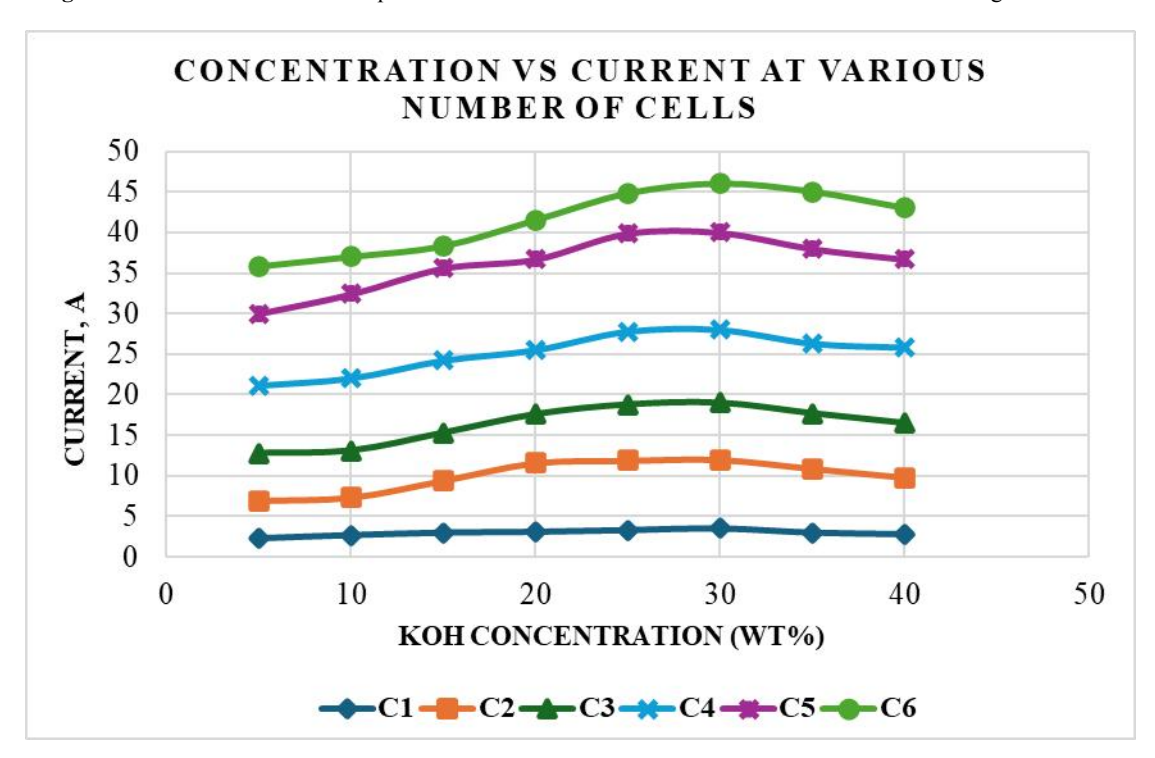


Figure 18: Behaviour of all cells at various concentrations as a function of flowing current.

In order to assess the reliability of the measurements, the statistical analysis would be performed. The mean value of the hydrogen production rate for each cell is shown in the figure 19, and the standard deviation of the mean is performed.

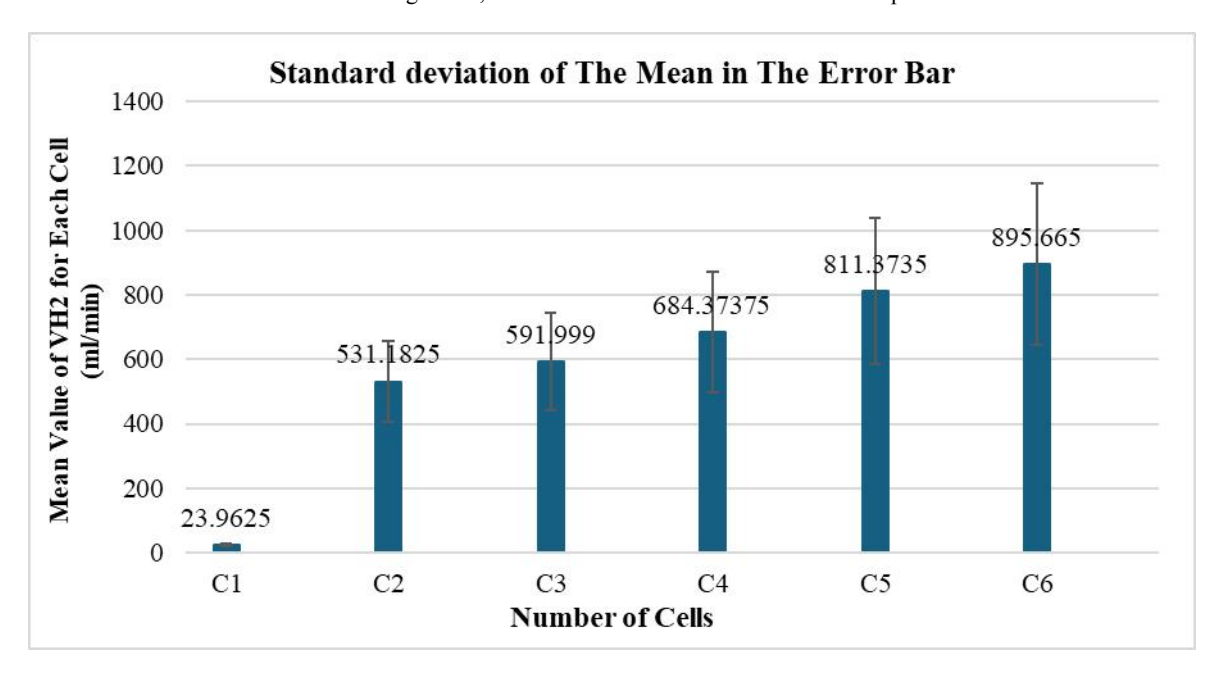


Figure 19: The mean values of the hydrogen production rate for each cell and the standard deviation of each mean.

Electrolyte temperature was measured during the experimental work at each concentration and recorded. It can be observed from figure 20 that, as the concentration increases, the electrolyte temperature increase. On the other hand, the 2C-3N perforated achieve a highest temperature value, which has 30.8 °C and 40.6 °C at 5 and 40 wt% respectively.

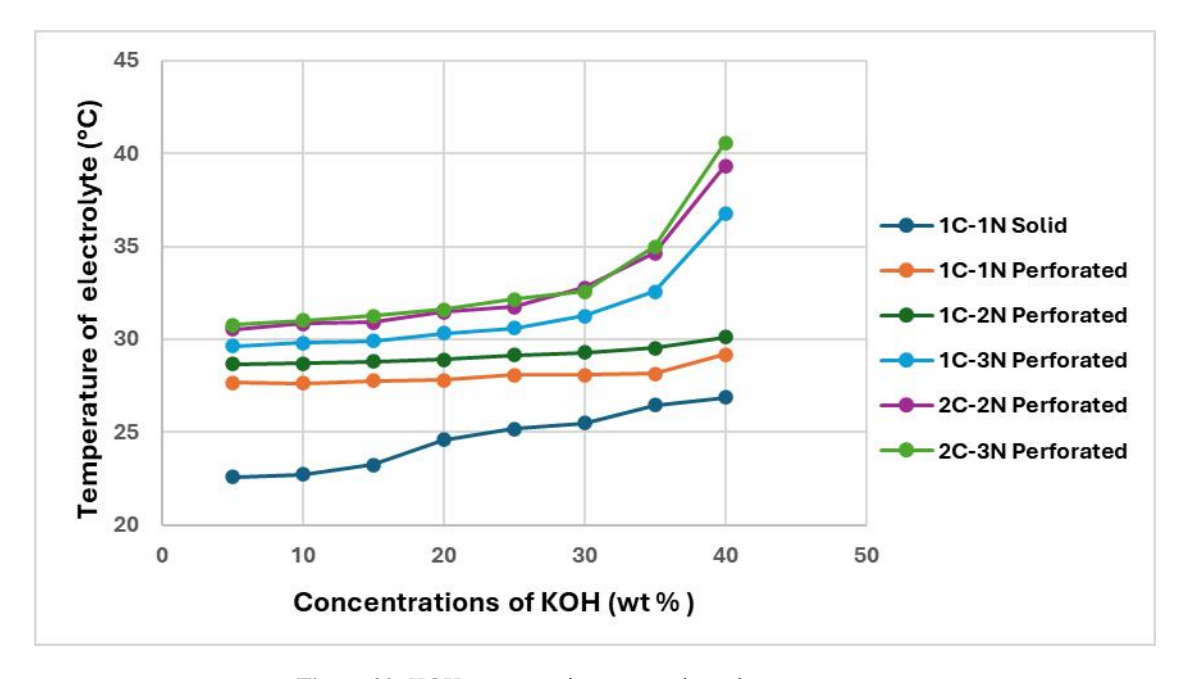


Figure 20: KOH concentration versus electrolyte temperature.

Power consumption will be calculated by multiplying the input voltage (12 volt) by the current flowing through the generator, where the current varies depending on the change in the KOH concentration in the electrolyte solution. Since the 2C-3N perforated cell achieved the better hydrogen production rate, therefore figure 21 shows power consumption versus its hydrogen production rate. The results show that at a rate of 1210 ml/min, the maximum power consumption reaches 552 Watt.

On the other hand, the specific energy consumption is determined by dividing the power consumption by the productivity of the HHO gas as shown in equation (6). Therefore, it can be concluded that as the productivity of the HHO gas increases, the power consumption increases.

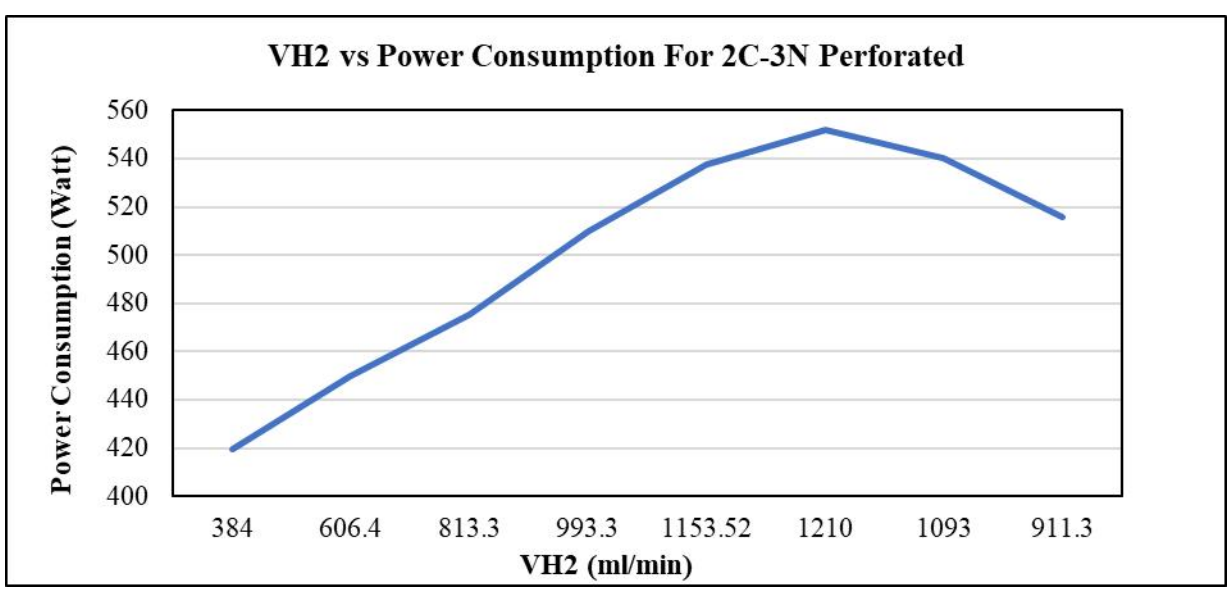


Figure 21: Hydrogen production rate versus power consumption for 2C-3N perforated cell.

Polarization resistance of the 316L SS immersed in KOH electrolyte solution for generating HHO gas from oxy-hydrogen generator is shown in figure 22. Results show that, i_corr is given as $0.1 \, (\mu A/cm^2)$, therefore, the corrosion rate value of the 316L SS is calculated from equation (13) which 1.14 $(\mu m/year)$.

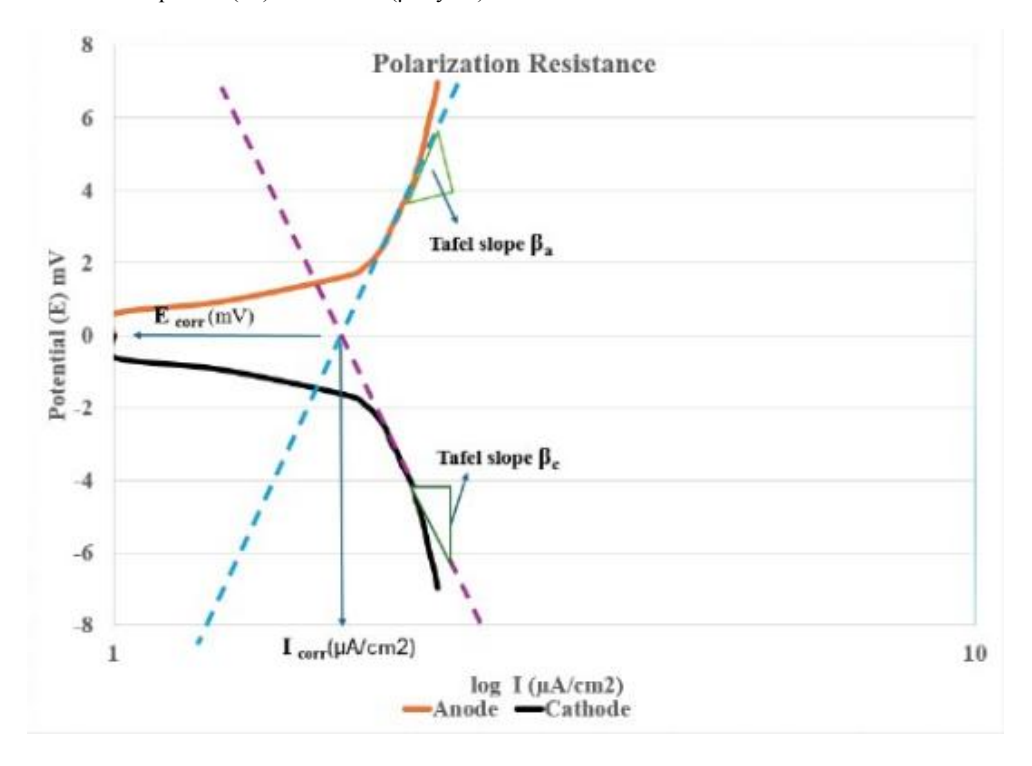


Figure 22: Experimental polarization curves for 316L SS in KOH solution.

4. Limitations in designing an HHO gas generator

Constructing and operating an HHO generator presents a range of interrelated technical, material, and operational challenges.

4.1. Electrode Degradation from Corrosion:

While 316L stainless steel is more resistant to corrosion than other grades, it's not completely immune to the corrosive effects of the KOH electrolyte, especially at higher temperatures and current densities which leads to reduced performance over the long-term.

4.2. Reduced Efficiency:

Corrosion products can deposit on the electrodes, reducing the effective surface area and hindering gas production. Higher current densities, while increasing gas production, can also lead to increased heat generation and electrolyte evaporation, decreasing overall efficiency. While higher temperatures can improve reaction kinetics, excessive heat can also lead to steam production, reducing the volume of HHO gas and lowering efficiency.

4.3. Electrolyte Contamination:

Iron ions from the corroding electrodes can contaminate the electrolyte, potentially affect its conductivity and further impact performance. Also, the deterioration of seals and gaskets, and electrode fouling reduced system efficiency and reliability.

4.4. Safety Concerns:

Explosive Gas:

HHO gas is highly flammable and can explode if ignited, especially at higher concentrations or pressures. All safety concerns should be taken in consideration while using HHO gas.

Flashback Risk:

The rapid combustion of HHO can lead to flashback, where the flame travels back into the generator, potentially causing damage or explosion. Therefore, flashback arrestor should be installed in the system outlet component

Pressure Buildup:

If the HHO gas is not properly vented, pressure can build up in the generator, increasing the risk of explosion.

4.5. Sealing and Leakage:

Proper sealing of the generator is crucial to prevent electrolyte leakage and ensure safe operation.

These limitations underscore the need for careful material selection, rigorous system design, and realistic expectations regarding the performance and application of HHO technology. In summary, while 316L stainless steel and KOH offer a reasonable starting point for HHO generation, careful consideration of these limitations is essential for designing a safe, efficient, and durable system.

5. Conclusion

The present work aimed to conduct experimental investigations on the influence of electrolyte concentration on the generation of oxyhydrogen gas. Therefore, the performance of several generators at different electrolyte concentrations of KOH solution in terms of HHO gas generation and flowing current at 12V is experimentally investigated. Several test runs are carried out for each cell separately, as each cell differs from the other according to the number of electrodes and perforated SS plates placed between electrodes to distribute the gas. It can be concluded that the perforated stainless steel current collector plates are more effective than solid plate that creates losses due to gas bubbles arise from hydrogen and oxygen bubbles. Consequently, the active sites on the electrodes will be blocked and the conductivity of the electrolyte solution is reduced. This means increasing the number of cells and perforated plates, resulting in the generation of more HHO gas. Therefore, the 2C-3N perforated cell is the best cell producing HHO gas in the studied system. Regarding the electrolyte concentration, the study proved that 30 wt% is the optimum value for generating the highest HHO gas flow rate of 1210 ml/min and the highest flowing current of 46 A from the 2C-3N perforated cell. But, when the concentration exceeds 30 wt%, the flow rate of HHO gas begins to decrease due to severe corrosion of electrodes. The model has been validated with previous work obtaining considerable satisfactory results.

6. Abbreviations

 $\begin{array}{lll} C & Number of Cells \\ CO & Carbon Monoxide \\ H_2SO4 & Sulphoric Acid \\ HC & Hydrocarbon \\ HHO & Oxy-Hydrogen \\ KOH & Potassium Hydroxide \\ \end{array}$

M Mole

N Number of Neutral Plates

NaCl Sodium Chloride

NaHCO₃ Sodium Bicarbonate NaOH Sodium Hydroxide

Q_g Productivity of HHO Gas Generator (L/min)

SS Stainless Steel
T Operating Time (min)
V_{HHO} Volume of HHO Gas (Liter)
wt% Concentration Percentage by Weight

7. Conflicts of interest

The authors declare that they have no conflicts of interest regarding this article.

8. Formatting of funding sources

The authors did not receive any funding.

9. Acknowledgments

This research was conducted at the National Research Centre, Dokki, Cairo, Egypt. Therefore, I would like to thank the work team, especially the colleagues in the Solar Energy Department, for their helpful assistance during the development research. Special thanks to Eng. Mohammed Helmy for his assistance in carrying out the experimental work.

10. Reference

- [1] Dr. V. R. Mamilla, K. S. R. Murthy, M.V. Krishna, T.S.S.S M. Swamy, A. Ramesh, M. U. Krishna, Production of Brown's Gas using Hydroxy Generator, International Journal of Engineering & Technology, 7 (4.5) (2018) 428-457, https://doi.org/10.14419/ijet.v7i4.5.20198.
- [2] B. Subramanian, & S. Ismail, Production and use of HHO gas in IC engines. Int. J. Hydrogen Energy, 43 (2018) 7140–7154, https://doi.org/10.1016/j.ijhydene.2018.02.120.
- [3] A. A. Al-Rousan, & S. A. Musmar, Effect of anodes-cathodes inter-distances of HHO fuel cell on gasoline engine performance operating by a blend of HHO. Int. J. Hydrogen Energy, 43 (2018) 19213–19221, https://doi.org/10.1016/j.ijhydene.2018.08.118.
- [4] T. Nabil, & M. M. Kh. Dawood, Enabling efficient use of oxy-hydrogen gas (HHO) in selected engineering applications; transportation and sustainable power generation. J. Clean. Prod., 237 (2019) 117798, https://doi.org/10.1016/j.jclepro.2019.117798
- [5]. A. M. M. M. Mousa, H. A. A. Sayed, Kh. A. M. Ali, N. S. Elkaoud & W. A. E. Mahmoud, Energy-conversion efficiency for producing oxy-hydrogen gas using a simple generator based on water electrolysis, Content courtesy of Springer Nature, terms of use apply. Rights reserved, (2024) 25312, https://doi.org/10.1038/s41598-024-73534-1.
- [6] H. H. El-Ghetany, M. A. Halawa, A. E. Mohammed (2025). 'Theoretical Study of a Water Electrolyzer System for a Green Hydrogen Production Performance Evaluation Prediction.', *Egyptian Journal of Chemistry*, 68(5), pp. 471-488. doi:10.21608/ejchem.2024.312122.10190
- [7] H. I. Lee, H.-S. Cho, M. Kim, J. H. Lee, Ch. Lee, S. Lee, S. Kim, Ch.-H. Kim, K. B. Yi and W.-Ch. Cho, The Structural Effect of Electrode Mesh on Hydrogen Evolution Reaction Performance for Alkaline Water Electrolysis, Frontiers in Chemistry, 9 (2021) 1-10, https://doi.org/10.3389/fchem.2021.787787.
- [8] S. Krishnan, Koning V, M. Th. de Groot, A. de Groot, P. G. Mendoza, M. Junginger, G. J. Kramer, Present and future cost of alkaline and PEM electrolyzer stacks, Int J Hydrogen Energy, 48 (2023) 32313–32330, https://doi.org/10.1016/j.ijhydene.2023.05.031.
- [9] K. Zeng, D. Zhang, Recent progress in alkaline water electrolysis for hydrogen production and applications, Progress in Energy and Combustion Science 36 (2010) 307–326, https://doi.org/10.1016/j.pecs.2009.11.002.
- [10] R. Phillips, Ch. W. Dunnill, Zero gap alkaline electrolysis cell design for renewable energy storage as hydrogen gas, Royal Society of Chemistry journal, 6 (2016) 100643–100651, https://doi.org/10.1039/c6ra22242k.
- [11] G. F. Swiegers, R. N. L. Terrett, G. Tsekouras, T. Tsuzuki, R. J. Pace, R. Stranger, The prospects of developing a highly energy-efficient water electrolyzer by eliminating or mitigating bubble effects, Royal Society of Chemistry journal, 5 (2021) 1280–1310, https://doi.org/10.1039/d0se01886d.
- [12] H. Vogt, The actual current density of gas-evolving electrodes—notes on the bubble coverage, Electrochimica Acta 78 (2012) 183–187, http://dx.doi.org/10.1016/j.electacta.2012.05.124.
- [13] H. Vogt, The incremental ohmic resistance caused by bubbles adhering to an electrode, journal of applied electrochemistry, 13 (1983) 87-88, DOI:10.1007/BF00615891.
- [14] X. Deng, F. Yang, Y. Li, J. Dang, M. Ouyang, Quantitative study on gas evolution effects under large current density in zero-gap alkaline water electrolyzers, J Power Sources 555 (2023) 232378, https://doi.org/10.1016/j.jpowsour.2022.232378.
- [15] M. T. de Groot, A.W. Vreman, Ohmic resistance in zero gap alkaline electrolysis with a Zirfon diaphragm, Electrochimica Acta 369 (2021) 137684, https://doi.org/10.1016/j.electacta.2020.137684.
- [16] J. Bleeker, C. V. Kasteren, J. R. V. Ommen, Gas bubble removal from a zero-gap alkaline electrolyser with a pressure swing and why foam electrodes might not be suitable at high current densities, International Journal of Hydrogen Energy 57 (2024) 1398–1407, https://doi.org/10.1016/j.ijhydene.2024.01.147.

- [17] J. W. Haverkort, and H. Rajaei, Voltage Losses in Zero-gap Alkaline Water Electrolysis, Journal of Power Sources 497 (2021) 229864, https://doi.org/10.1016/j.jpowsour.2021.229864.
- [18] M. T. de Groot, and A. W. Vreman, Ohmic Resistance in Zero gap Alkaline Electrolysis with a Zirfon Diaphragm. Electrochimica Acta 369 (2021) 137684, https://doi.org/10.1016/j.electacta.2020.137684.
- [19] X. G. Jiang, Y. P. Zhang, C. Song, Y. C. Xie, T. K. Liu, C. M. Deng, N. N. Zhang, et al. (2020). Performance of Nickel Electrode for Alkaline Water Electrolysis Prepared by High Pressure Cold spray, International Journal of Hydrogen Energy, 45 (2020) 33007-33015, https://doi.org/10.1016/j.ijhydene.2020.09.022.
- [20] H. I. Lee, M. Mehdi, S. K. Kim, H. S. Cho, M. J. Kim, W. Ch.Cho, Y. W. Rhee, and Ch. H. Kim, et al. (2020). Advanced Zirfon-type Porous Separator for a High-Rate Alkaline Electrolyzer Operating in a Dynamic Mode, Journal of Membrane Science 616 (2020) 118541, https://doi.org/10.1016/j.memsci.2020.118541.
- [21] B. Zayat, D. Mitra, A. Irshad, A. S. Rajan, and S. R. Narayanan, Inexpensive and Robust Iron-Based Electrode Substrates for Water Electrolysis and Energy Storage. Curr. Opin. Electrochemistry 25 (2021) 100628, https://doi.org/10.1016/j.coelec.2020.08.010.
- [22] S. G. Nnabuife, C. K. Darco, P. Ch. Obiako, B. Kuang, S. Sun, K. Jenkins, A Comparative Analysis of Different Hydrogen Production Methods and Their Environmental Impact. Clean Technol, 5 (2023) 1344–1380, https://doi.org/10.3390/cleantechnol5040067.
- [23] V. S. S. Muthu, Sh. A. Osman, & S. A. Osman, A review of the effects of plate configurations and electrolyte strength on production of brown gas using dry cell oxy-hydrogen generator. J. Adv. Res. Fluid. Mech. Therm. Sci., 99 (2022) 1–8, https://doi.org/10.37934/arfmts.99.1.18.
- [24] P. Indah, W. Noorsakti, A. F. Yoga, P. W. Galih, Design of Generator HHO Dry Cell Type and Application on 110 Cc Engined Vehicles Towards Gas Emissions, J. Phys.: Conf. Ser., 1845 (2021) 012002, https://doi.org/10.1088/1742-6596/1845/1/012002.
- [25] N. N. Patil, C B Chavan, A. S More and P Baskar, Generation of oxy hydrogen gas and its effect on performance of spark ignition engine, IOP Conf. Series: Materials Science and Engineering 263 (2017) 062036, doi:10.1088/1757-899X/263/6/062036.
- [26] A. Zaki, "Principle of Corrosion Engineering and Corrosion Control", IChemE, Butterworth-Heinemann/Elsevier, Amsterdam, 2006, https://doi.org/10.1016/B978-0-7506-5924-6.X5000-4.
- [27] M. W. S. Jawich, " A Sudy of Amidoamines as Inhibitors For Mild Steel Corrosion in Saline Media Saturated with Carbon Dioxide" King Fahd University of Petrolume & Minerals, Dhahran, Saudi Arabia, Thesis, May 2011.
- [28] B. Basori, W. M. F. W. Mohamad, M. R. Mansor, N. Tamaldin, A. Iswadi, M. K. Ajiriyanto and F. B. Susetyo, "Effect of KOH concentration on corrosion behavior and surface morphology of stainless steel 316L for HHO generator application", J. Electrochem. Sci. Eng. 13(3) (2023) 451-467; http://dx.doi.org/10.5599/jese.1615.
- [29] A. Ramadan, E. El-Shenawy, A. Abdel Dayem and T. F, A. Optimization of PV-Hydrogen Electrolyzes System, January 2011, Conference: AAST, DOI: 10.21608/asat.2011.23400.